Australian Dental Journal
The official journal of the Australian Dental Association

Australian Dental Journal 2012; 57:(1 Suppl): 46–60

doi: 10.1111/j.1834-7819.2011.01657.x

Maxillofacial cone beam computed tomography: essence, elements and steps to interpretation

WC Scarfe,* Z Li,† W Aboelmaaty,‡ SA Scott,§ AG Farman¶

*Professor, Radiology and Imaging Science Division, Department of Surgical and Hospital Dentistry, School of Dentistry, The University of Louisville, Kentucky, USA.
†Visiting Research Scholar at the University of Louisville from the Department of Oral Radiology, Jilin University School and Hospital of Stomatology, Chang Chun, Jilin Province, China.
‡Visiting Research Scholar at the University of Louisville from the Department of Oral Medicine and Periodontology, Faculty of Dentistry, Mansoura University, Egypt.
§Associate Professor, Department of Anatomical Sciences and Neurobiology, School of Medicine, The University of Louisville, Kentucky, USA.
¶Professor, Radiology and Imaging Science Division, Department of Surgical and Hospital Dentistry, School of Dentistry and Adjunct Professor in the Department of Anatomical Sciences and Neurobiology, School of Medicine, The University of Louisville, Kentucky, USA.

ABSTRACT

Maxillofacial cone beam computed tomography (CBCT) is one of the most significant advances in dental imaging since rotational panoramic radiography. While the acquisition of CBCT data is technically simple, numerous parameters should be considered so that CBCT imaging is performed appropriately and 'task specific'. This involves an understanding of not only exposure (e.g. geometric and software parameters to minimize patient dose, while sustaining diagnostic image quality) but also image formatting options to maximize image display. CBCT images contain far more detailed information of the maxillofacial region than do panoramic or other 2-D images and necessitate a thorough knowledge of the 3-D anatomy of the region and considerations of variability in the range of the anatomically normal. These principles, procedures and protocols, together with the interpretation of CBCT images form the basis of best practices in maxillofacial CBCT imaging. This communication aims to provide: (1) an overview of the fundamental principles of operation of maxillofacial CBCT technology; (2) an understanding of 'task specific' equipment, image selection and image display modes; and (3) a systematic methodology for sequencing interpretation of CBCT images.

Keywords: 3-D X-ray, computed tomography, X-ray, cone beam, dental radiography, diagnostic image processing.

Abbreviations and acronyms: ALARA = As Low As Reasonably Achievable; CAT = computed axial tomography; CBCT = cone beam computed tomography; CMOS = complementary metal oxide semiconductor technology; CT = computed tomography; DVR = direct volume rendering; FDK = Feldkamp; FH = Frankfort horizontal; FOV = field of view; FPD = flat panel detectors; HU = Hounsfield units; II/CCD = image intensifiers and charge-coupled device; IVR = indirect volume rendering; kV = kilovolt; mA = milliampere; MIP = maximum intensity projection; MPR = multiplanar reformations; MSCT = multiple slice detector acquisition; ROI = region of interest; RPR = rotational panoramic radiography; TACT = tuned aperture computed tomography.

INTRODUCTION

Diagnostic imaging is an important adjunct to clinical assessment of the dental patient. Historically, this has been accomplished by intra or extraoral projection radiography, the latter including rotational panoramic radiography. These techniques are based on the transmission, tissue attenuation and recording of residual X-rays on a single planar medium (either analogue film or a digital receptor). Accurate image formation is based on the optimal geometric configuration of the X-ray generator, patient and sensor during the activation of the X-ray generator. The image produced is limited to a two-dimensional (2-D) representation of a three-dimensional (3-D) object. If any component of the imaging chain is compromised, then the image may demonstrate exposure or geometric errors and be suboptimal for the diagnostic task in hand.

In dentistry, several imaging technologies have been tried for volumetric imaging capability including stereoscopy, tomography, tomosynthesis and tuned aperture computed tomography (TACT).[1,2] In 1972, the independent findings of Hounsfield and Cormack revolutionized medical diagnostic imaging with the invention of the computed tomography (CT) scanner.[3,4] This device images a subject using an X-ray tube rigidly linked to a detector located on the other side of the subject. Together the tube and the detector scan across the subject, sweeping a narrow X-ray beam through one thin slice at a time. Reconstruction of the transmitted X-ray attenuation data by specific software algorithms produces adjacent image slices of the imaged volume, usually in the axial plane, perpendicular to the long axis of the object; hence the term computed axial tomography, or 'CAT' scan.[5] CT acquisition has subsequently been refined to incorporate a helical or spiral synchronous motion, fan-shaped beam and multiple slice detector acquisition (MSCT) enabling fast scan times and providing high quality images which can be integrated to produce a volumetric dataset (Fig. 1). While CT has been available for many years, its clinical application in dentistry has been limited because of equipment cost, access and radiation dose considerations.

An early volumetric CT predecessor of cone beam computed tomography (CBCT), the Dynamic Spatial Reconstructor, was developed in the late 1970s by the Biodynamics Research Unit at the Mayo Clinic.[6] Subsequently applied for vascular imaging,[7] CBCT prototypes based upon C-arms were demonstrated as early as 1983. CBCT provided an alternate method of image production, allowing more rapid acquisition of data for a region of interest (ROI) using a comparatively less expensive radiation detector than conventional CT. Unlike conventional CT, which uses limited beam geometry and measures attenuation, CBCT uses a divergent conical- or, more recently, pyramidal-shaped source of ionizing radiation and an area detector to provide multiple transmission images that are integrated directly forming volumetric information (Fig. 1).[8–11] CBCT is not a modality specific to dentistry.

Four technological developments converged to facilitate construction of affordable CBCT units small enough to be used in the dental office for maxillofacial imaging: the introduction of X-ray detectors capable of rapid acquisition of multiple basis images; development of suitably resilient X-ray generators; evolution of suitable image acquisition and integration algorithms;[12–14] and the availability of computers powerful enough to process the enormous amount of acquired image data. The technology transfer of CBCT to dentistry first occurred in 1995. Italian co-inventors Attilio Tacconi and Piero Mozzo developed a CBCT system for the maxillofacial region that was designed and produced by QR Inc. of Verona. This unit, the NewTom DVT 9000 (Maxiscan in Italy only, branded by Esaote) became the first commercial CBCT unit, initially introduced in Europe in 1999.

The introduction of CBCT has heralded a shift from a 2-D to a volumetric approach in maxillofacial imaging in terms of technical data acquisition, reconstruction, image display and image interpretation.[11] The rapid adoption of volumetric imaging by various disciplines of dentistry has occurred because CBCT provides a cost-effective diagnostic technology[15] with expanding applications in treatment planning and image guidance of operative and surgical procedures.[16]

Fundamental principles of CBCT imaging

There are two main components to CBCT imaging, namely, image production and image display.

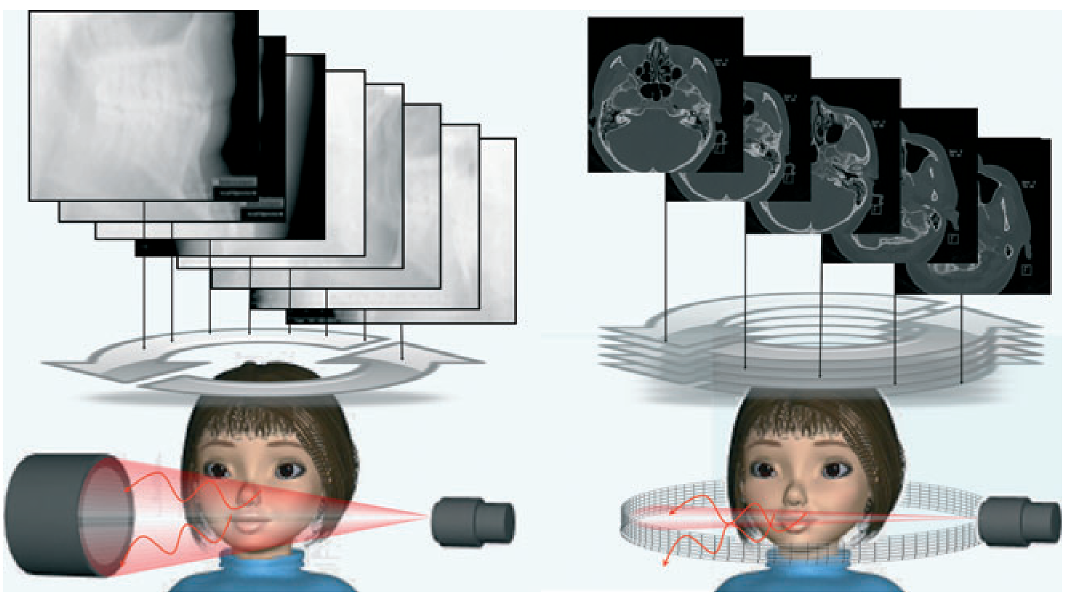

Fig 1. X-ray beam projection scheme comparing acquisition geometry of cone beam imaging (left) with conventional 'fan beam' CT (right). In cone beam geometry, multiple basis projections form the projection data from which orthogonal planar images are secondarily reconstructed. In fan beam geometry, primary reconstruction of data produces axial slices from which secondary reconstruction generates orthogonal images. The amount of scatter generated and recorded by cone beam image acquisition is substantially higher, reducing image contrast and increasing image noise.

Image production

The production of CBCT images is accomplished in three consecutive phases:

(1) **Acquisition configuration.** The geometric configuration and acquisition mechanics for the CBCT technique are theoretically simple (Fig. 1). CBCT imaging is performed using a rotating platform or *gantry* to which an X-ray source and detector are fixed. A divergent pyramidal- or cone-shaped source of ionizing radiation (similar in shape to the divergent beam of traditional 2-D transmission imaging) is directed through the middle of the ROI and the transmitted, attenuated radiation is projected onto an area X-ray detector on the opposite side. The X-ray source and detector rotate around a fulcrum, fixed within the centre of the ROI. This fulcrum acts as the centre of the final acquired volume imaged. During the rotation, multiple sequential planar projection images covered by the detector or the field of view (FOV) are acquired in an arc of 180° or greater. These single projection images constitute the raw primary data and are individually referred to as *basis, frame* or *raw* images. Basis images appear similar to cephalometric radiographic images, only each is slightly offset from the next. There are usually several hundred 2-D basis images from which the image volume is calculated and constructed. The complete series of images is referred to as the *projection data*. This varies from a traditional medical CT as the latter uses a fan-shaped X-ray beam in a helical progression acquiring individual or groups of image slices of the FOV and then, subsequently, stacks the slices to obtain a volumetric representation (Fig. 1). Because CBCT exposure incorporates the entire FOV, only one rotational sequence of the gantry of 180° or greater is necessary to acquire enough data for volumetric image construction.

For CBCT, X-ray generation may be continuous or pulsed to coincide with the detector activation. Pulsed X-ray beam generation is preferable as it results in less radiation dosage to the patient.

The dimensions of the FOV or *scan volume* depend on the detector size and shape, beam projection geometry and the ability to collimate the beam. The shape of the scan volume can be either a cylinder (e.g. iCAT Next Generation, Imaging Sciences International, Hatfield, PA, USA) or spherical (e.g. NewTom 3G, Quantitative Radiology, Verona, Italy). As much of the manufacturing expense of CBCT units is from the cost of the X-ray detector, two approaches have been introduced to enable scanning of a ROI greater than the FOV of the detector. The first method involves obtaining data from two or more separate scans, superimposing overlapping CBCT data volumes using corresponding fiducial reference landmarks (referred to as either 'bio-image registration' or 'mosaicing') and fusing adjacent image volumes ('stitching' or 'blending') to create a larger volumetric dataset, either in the horizontal or in the vertical dimension (Fig. 2). This

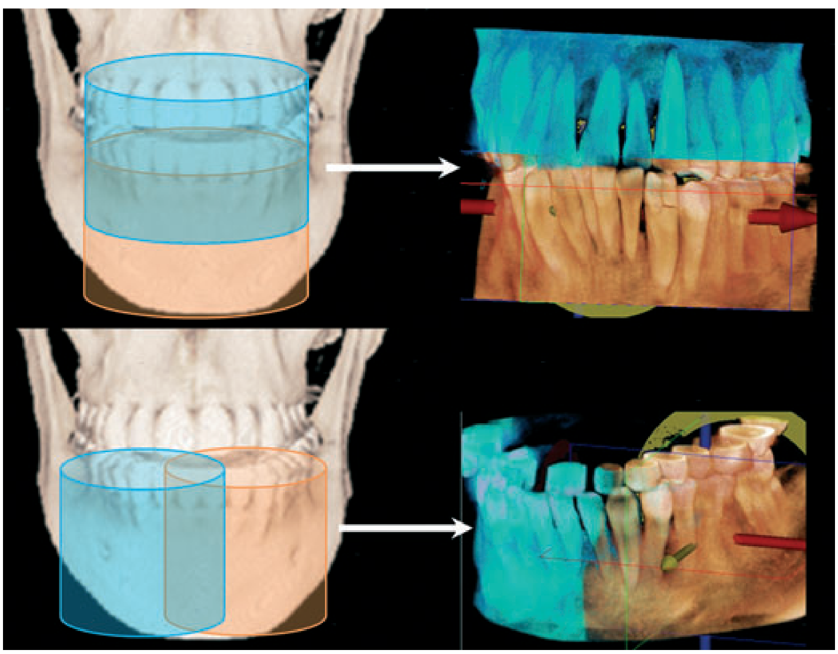

Fig 2. Larger regions of interest can be acquired by fixed small FOV CBCT units by 'stitching' adjacent limited area volumetric datasets. This process requires acquisition of separate scans (left), registration of each volume by superimposition of fiducial landmarks and fusion to provide a larger FOV (right). The proprietary software of many CBCT units provide this function automatically to increase either the vertical (top) or horizontal (lower) FOV. Shown here are adjacent (orange and blue) volumetric datasets obtained from the KODAK 9000 DS stitched manually using InVivoDental software (Anatomage, San Jose, CA, USA).

process can be accomplished manually using third-party imaging and analysis software (e.g. InVivoDental, Anatomage, San Jose, CA, USA) or automatically by proprietary software provided by the CBCT system manufacturer or vendor. Bundled automatic stitching can be vertical (e.g. Romexis Stitching Program, Planmeca Oy, Helsinki, Finland) or horizontal (Kodak Dental Imaging Software, Carestream Dental, Atlanta, GA, USA). The disadvantage of stitching overlapped regions is that such overlapped regions are imaged twice (i.e. *over scanned*), resulting in doubling the radiation dose to such regions. A second method to increase the height or width of the FOV using a smaller area detector is to offset the position of the detector, collimate the beam asymmetrically and scan only half the patient's ROI in each of the two offset positions (e.g. iCAT Next Generation for the full cranio-maxillofacial scan mode; and Scanora 3D, SOREDEX, Tuusula, Finland).

Data reconstruction in CBCT with complete information content requires the acquisition of projection basis images from a circular trajectory scan arc of 180° or greater. The image quality is determined to some extent by the number of samples (i.e. basis images) recorded and increased sampling is sometimes achieved by a 360° or even a 720° rotation. It is mechanically difficult to fabricate a robotic platform capable of achieving a 360° or greater rotation arc for CBCT X-ray generator/detector geometry if the CBCT design is based upon an existing dental panoramic machine structural platform, so a number of CBCT units (e.g. Galileos, Sirona AG, Bensheim, Germany; and Promax 3D, Planmeca Oy, Helsinki, Finland) use shorter rotation arcs.

The number of images comprising the projection data throughout the scan is determined by the *frame rate* (number of images acquired per second), the completeness of the trajectory arc and the speed of the rotation.

(2) **Image detection.** Detectors were initially produced using a configuration of image intensifiers and charge-coupled-device (II/CCD) detectors. II/CCD detectors, still used by some manufacturers, are large and bulky and most frequently result in circular basis image areas (spherical volumes) rather than rectangular ones (cylindrical volumes). Now most, but not all, CBCTs use flat panel detectors (FPD) comprising a large area pixel array of hydrogenated amorphous silicon thin-film transistors, or in some cases more recently large complementary metal oxide semiconductor technology (CMOS) arrays. In both FPD circumstances, X-rays usually are detected indirectly by means of a scintillator such as thallium doped cesium iodide or terbium activated gadolinium oxysulphide, converting them to visible light that is registered in the photo diode array. FPD are less complicated, less bulky and offer greater dynamic range than II/CCD detectors. For each basis image, the detector records incident X-ray photons, collects a charge and sends a signal to the computer. As rotation is usually performed within times equivalent or less compared to panoramic radiography (from approximately 5 seconds to usually <20 seconds), this means that each basis image is acquired and sent within milliseconds, and this occurs many hundreds of times within a single exposure rotation. The speed with which a detector performs this acquisition is called the *frame rate*. Unfortunately, FPD have limitations in their performance including linearity of response to the radiation spectrum, lack of uniformity of response throughout the area of the detector and bad-pixels. The effects of these on image quality are most noticeable at lower and higher exposures. To overcome this, detectors should be recalibrated periodically.

The resolution and therefore detail of CBCT imaging is determined by the individual volume elements or *voxels* produced in formation of the volumetric dataset. In CBCT imaging, voxel dimensions are primarily dependent on the pixel size on the area detector, not as with conventional CT, on slice thickness. Detectors with smaller pixels capture less X-ray photons and result in more image noise. Consequently, CBCT imaging using higher resolutions may be designed to use higher dosages to achieve a reasonable signal-to-noise ratio for diagnostic image quality.[17] However, the selected voxel dimensions are not invariably associated with change in dose. Key factors related to dose are time sequence, exposure parameters (mA and kV), collimation and filtration.

(3) **Image reconstruction.** The native, raw data from CBCT acquisition is a series from approximately 100 to over 600 individual 2-D projection frames (basis images) each with over a million pixels with 12- to 16-bits of data assigned to each pixel. This data is then processed to create a volumetric dataset composed of cuboidal volume elements (voxels) by sequence of software algorithms in a process called *reconstruction* (Fig. 3). Subsequent orthogonal images are secondarily generated from the volumetric dataset. Reconstruction times vary depending on the acquisition parameters (voxel size, FOV, number of projections), hardware (processing speed, data throughput from acquisition to workstation computer) and software (reconstruction algorithms) used.

The reconstruction process consists of two stages, each comprising numerous steps:

(a) **Acquisition stage** (Fig. 4). Because of limitations in X-ray detection and registration, raw images from CBCT detectors innately demonstrate variations of both dark image offset and pixel gain as well as pixel imperfections. Dark image offset is the accumulation of charge by the detector while it is idle, whereas gain is due to variations in sensitivity across the detector. To compensate for the resulting inhomogeneities, raw

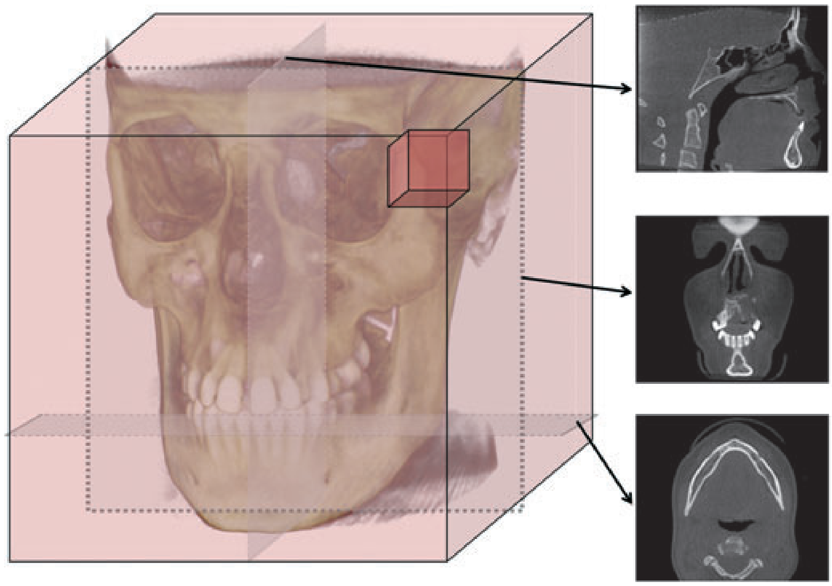

Fig 3. CBCT volumetric dataset. As CBCT data acquisition is dependent on the pixel size of the area detector and not on the acquisition of groups of rows with sequential translational motion that is the case in conventional MSCT, the compositional voxels are equal in all three dimensions rather than columnar. Initial display images are secondarily reconstructed from the dataset at three right angle planes (orthogonal).

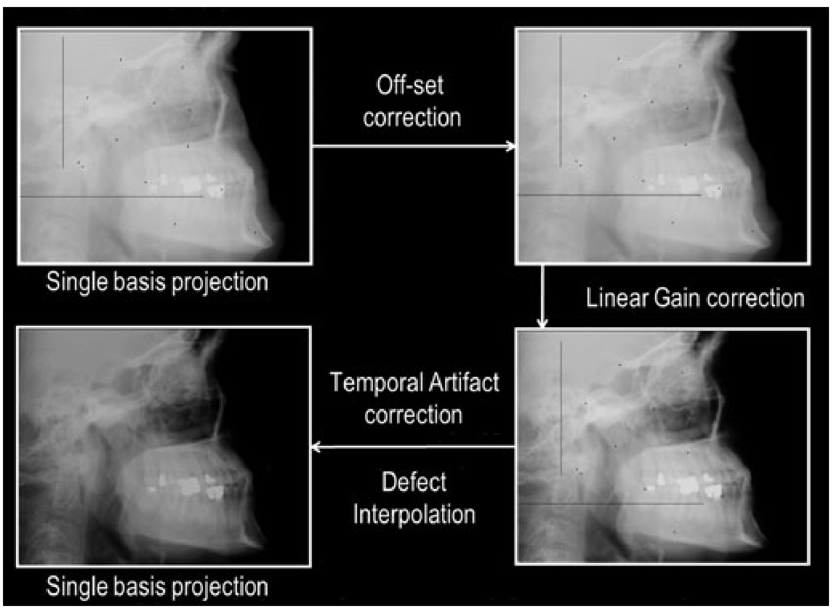

Fig 4. CBCT detector preprocessing. The first step of the detector preprocessing is the offset correction, which is performed by pixel-wise subtraction of an individual offset value computed by averaging over a series of up to 30 dark images. The second step is the linear gain calibration consisting of dividing each pixel by its individual gain factor. The gain factors are obtained by averaging a sequence, again with up to 30 images, of homogeneous exposures without any object between X-ray source and detector. The gain sequence is first offset corrected with its own sequence of dark images. The next procedure is the defect interpolation. Each pixel that shows unusual behaviour, either in the gain image or in the average dark sequence, is marked in a defect map. The grey values of pixels classified as defective in this way are computed by linear interpolation along the least gradient descent. For flat detectors there is usually an additional procedure to correct for temporal artefacts. These arise in flat detectors because both the scintillator and the photodiodes exhibit residual signals.

images require systematic offset and gain calibration as well as a correction to help hide defective pixels. The sequence of the required calibration steps is referred to as detector *pre-processing* and requires the acquisition of additional image sequences.

(b) **Reconstruction stage.** Once images are corrected, they are converted into a special representation called a sinogram, corrected and then processed by reconstruction filter algorithm. The most widely used filtered back projection algorithm for cone beam acquired volumetric data is the Feldkamp (FDK) algorithm.[12] Once all sinograms have been reconstructed, they can be recombined into a single volume for visualization.

Image acquisition settings, image quality and dose

Operation of CBCT equipment is technically simple and similar, in many respects, to the performance of rotational panoramic radiography (RPR) – the patient is placed within the unit, the head stabilized and the apparatus rotates around the patient's head. However, unlike RPR where the operator is usually only able to adjust the kV depending on patient head size, numerous image acquisition settings may be adjusted, depending on the CBCT unit used. Practitioners and operators using CBCT must have a thorough understanding of the operational parameters and the effects of these parameters on image quality and radiation safety.[18]

Exposure settings

The quality and quantity of the X-ray beam is dependent on the potential difference, referred to as kilovoltage (kV), and the current, measured in milliamperes (mA). CBCT manufacturers approach setting exposure factors in one of two ways.[19] They either provide a selection of 'fixed' exposure settings (e.g. i-CAT; and NewTom 3G) or allow operator 'manual' adjustment of kV and/or mA (e.g. MercuRay CB; Hitachi Medical System America, Twinbury, OH, USA; and Accuitomo, Morita, Kyoto, Japan). Operators who use CBCT units with operator adjustable exposure settings must understand that these parameters affect both image quality (Fig. 5) and patient radiation dose, and hence careful selection is required to fulfil the ALARA (As Low As Reasonably Achievable) principle.[20] While mA may be increased on some units and is suggested to compensate for increases in patient size, the effective dose increases proportionately, almost in a 1:1 ratio.[21] Adjustment of kV has an even greater affect on dose than does mA, with each increase in 5 kV approximately doubling dose if all other parameters remain the same. Exposure parameters should be appropriate for both the given patient size and to the diagnostic task that motivated image selection. Dental periapical diagnosis involving discernment of the periodontal ligament space and subtle changes in bone trabeculation has been found to require higher exposure parameters as compared to implant planning.[22] In addition, it is reported that significant dose reductions can be achieved by reducing tube current by up to 50% without substantial loss of diagnostic quality for relatively low-resolution tasks such as pre-surgical implant planning[23] or orthodontic diagnosis.[24]

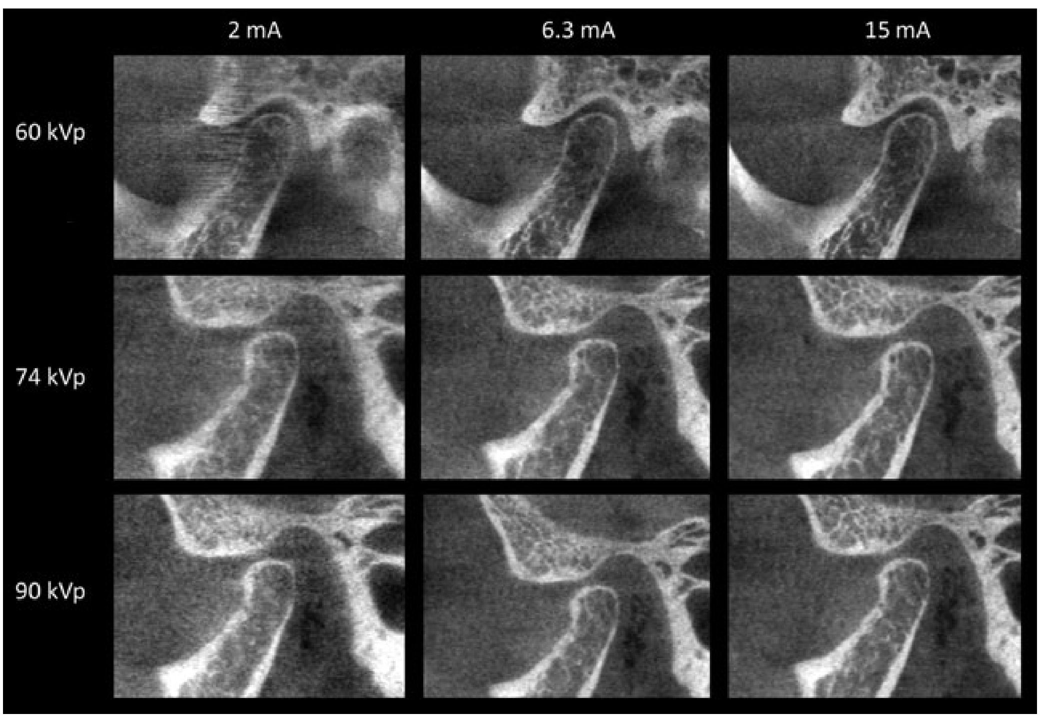

Fig 5. Representative 0.076 mm para-sagittal slices of the left temporomandibular joint of a cadaver demonstrating the effect of changing mA (rows) and kVp (columns) on image quality for low (cortical cone) and high (cancellous bone) diagnostic tasks. Images are adequate for visualization of gross morphologic changes at all values. However, at low kVp and mA there is increased graininess (noise) of the images making discernment of the fine trabecular pattern within the cancellous bone or surface irregularities of the condylar cortical plate more difficult. Little improvement in subjective image quality is achieved at settings greater than 74 kVp and 6.3 mA despite appreciable associated increases in dose. Images acquired with a KODAK Dental Imaging 9000 DS (Carestream Health Dental Imaging/Practiceworks, Atlanta, GA, USA).

Image resolution

There are two types of resolution – spatial resolution determining the proximity of details able to be recorded separately and contrast resolution, enabling distinction between tissues of different radio-density. Spatial resolution is moot when contrast is insufficient to differentiate between tissue densities of the adjacent structures concerned.

Spatial resolution

CBCT units in general provide voxel resolutions that are *isotropic* – equal in all three orthogonal dimensions (Fig. 3) – unlike the spatial resolution of many conventional CT images in which the resolution along the axial or scanning direction is sometimes significantly lower than in the transverse direction, referred to as *anisotropic*. While spatial resolution of CBCT systems is primarily a function of detector nominal pixel size, factors such as beam projection geometry, patient scatter, detector motion blur and fill factor, focal spot size, number of basis images and reconstruction algorithm all contribute to the final maximum achievable resolution.[25] Some manufacturers provide user options for varying acquisition resolution of CBCT data. As detectors cannot, *per se*, be altered to change the number of pixels within the area matrix that capture X-rays, electronic *pixel binning* is used to provide images with resolution less than that acquired. Pixel binning is the process of combining charge from adjacent pixels from the detector during readout. The two primary benefits of binning are improved contrast due to an improved signal-to-noise ratio and the ability to increase frame rate, albeit at the expense of reduced spatial resolution. While higher resolution may be considered desirable for many tasks in dentistry, it should be used judiciously for procedures demanding accuracy to the level of the detail of approximately the periodontal ligament space (i.e. approximately 0.2 mm or less). Images taken at high resolution often have reduced brightness and contrast, increased noise and require increased reconstruction time (Fig. 6). While increased image resolution in some CBCT units does not affect changes in exposure parameters, some manufacturers incorporate reduced-dose exposure protocols for low-resolution settings.[21]

As with other forms of digital radiography, care should be taken to distinguish between theoretical spatial resolution based on specified theoretical pixel or voxel values and the actual resolution achieved due to the various constraints within the total imaging chain.

Contrast resolution

Several factors limit the contrast resolution of CBCT. The inherent geometric configuration of image acqui-

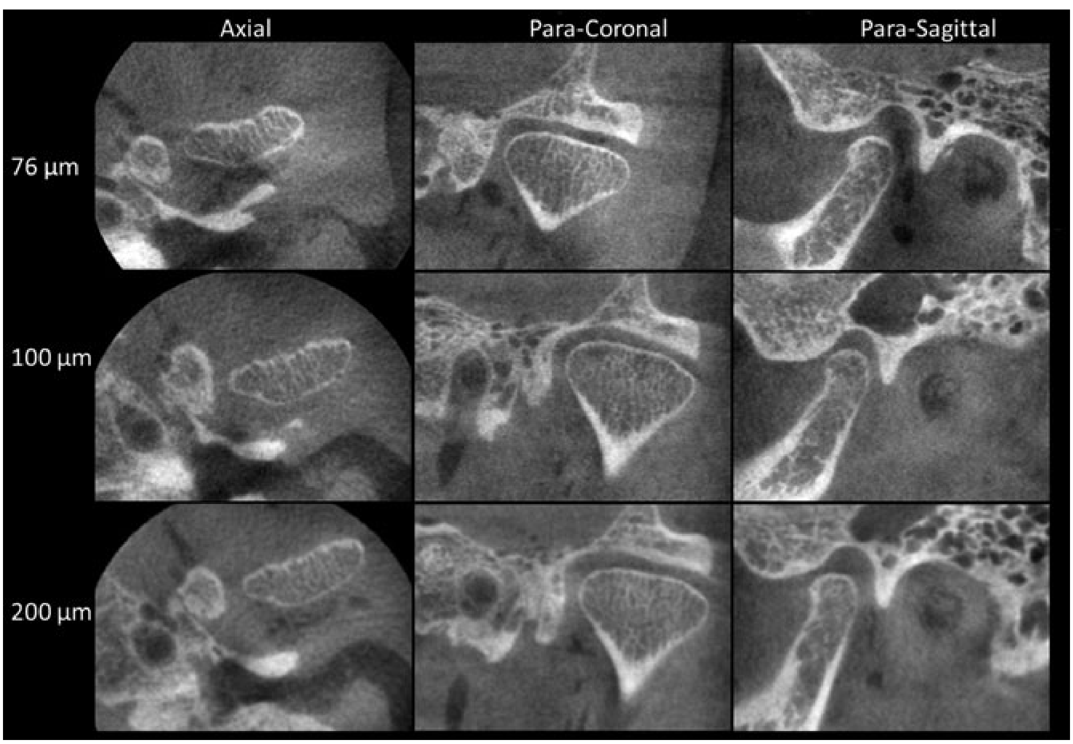

Fig 6. Representative orthogonal (axial [left], para-coronal [centre] and para-sagittal [right]) sections of cadaver left temporomandibular joint (74 kVp, 6.3 mA) demonstrating effect of increasing resolution on image quality for low (cortical cone) and high (cancellous bone) diagnostic tasks. Note that at higher resolutions cortical and cancellous bone characteristics become smoother or slightly more blurred, demonstrating the effect of decreased noise. Images acquired with a KODAK Dental Imaging 9000 DS (Carestream Health Dental Imaging/Practiceworks, Atlanta, GA, USA).

sition involving an area detector to register attenuated primary radiation from a cone source produces significant scatter radiation. This contributes to increased noise of the image as well as being a significant factor in reducing the contrast of any CBCT system. In addition, because of the divergence of the X-ray beam over the area detector, there is a large variation or non-uniformity of the incident X-ray beam on the patient. Subsequently, there is resultant non-uniformity in absorption on the area detector, with greater signal-to-noise ratio (noise) on the cathode side of the image relative to the anode side (heel effect). Further, numerous inherent FPD-based artefacts – or those associated with image intensifiers when such are employed – affect linearity in response to X-radiation. For these reasons, and the reduced kV and mA of CBCT compared to MSCT, maxillofacial CBCT images lack adequate grey scale sensitivity to discern subtle differences between soft tissues, such as between fluids and solid tumours. In addition, greyscale intensity values measured on CBCT images do not directly represent Hounsfield units (HU), the relative density of body tissues according to a calibrated grey-level scale, based on normalized-HU values for air (−1000 HU), water (0 HU), and dense bone (+1000 HU).[26,27] While these conditions limit the application of current maxillofacial CBCT imaging to the assessment of osseous structures, several techniques and devices are currently being investigated to suppress these effects or derive HU from grey levels in dental CBCT.[28–30] Further, CBCT can be designed specifically for soft tissue differentiation and employed in such domains as cardiology and for mammography. The detector configurations, exposure parameters and algorithms differ from those employed for maxillofacial CBCT.

Maxillofacial CBCT imaging provides adequate spatial and contrast resolution to demonstrate the detail of osseous structures. However, CBCT is compromised by image artefacts due to image acquisition (e.g. beam hardening producing scatter streaks and dark bands) (Fig. 7), patient-related artefacts (e.g. patient motion leading to unsharpness), the scanner itself (e.g. ring artefacts) or the cone/pyramidal beam projection geometry (e.g. distorted periphery). Beam hardening artefacts in particular, make CBCT imaging unsuitable for dental caries diagnosis, especially in restored dentitions. CBCT imaging should be considered as a complementary modality for specific applications, not as a replacement technology for all other radiographic methods.

Frame rate

The number of projection scans comprising a single scan may be fixed (e.g. Newtom 3G; Iluma, Ardmore, OK, USA; Galileos; or Promax 3D) or variable (e.g. iCAT; or PreXion 3D, TeraRecon, San Mateo, CA, USA). More projection data provides more information to reconstruct the image, allows for greater spatial and contrast resolution, increases the signal-to-noise ratio producing 'smoother' images, and reduces metallic artefacts. However, this is usually accomplished with a longer scan time, with a proportionally higher patient dose[31] and longer primary reconstruction time. There is a dearth of literature specifically on the effects of the number of basis projections, independent of other adjustments, on diagnostic image quality for maxillofacial CBCT.

Trajectory arc

While most CBCT units have fixed scan arcs, some units provide a choice of manual controls to reduce this further. This reduces the scan time and patient radiation dose. However, images produced by this method may have greater noise and suffer from reconstruction interpolation artefacts depending on the number of basis images interpolated for the reconstruction. Reduction of scan arc from 360° to 180° with an accompanying 50% reduction in patient radiation dose has been reported to produce images of adequate diagnostic quality for implant planning in the upper jaw.[23] Reductions in exposure arcs below 180° result in incomplete information, and theoretically in loss of

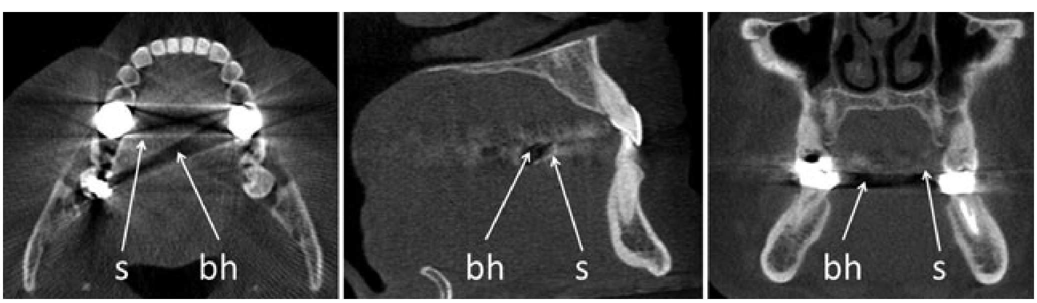

Fig 7. Axial (A), mid-sagittal (B) and coronal (C) CBCT images demonstrating the effects of scatter (s) and beam hardening (bh) due to the presence of metallic restorations on image quality producing linear high density linear (opaque) and low density (void) streak artefacts respectively.

image quality. Secondary reduction in image basis images to exclude those attained during patient motion has been suggested as a possible means to improve diagnostic image quality; however, this requires further investigation of impact on diagnostic quality.

Field of view

Only a few CBCT units are now produced that have a fixed FOV. Reduction in the FOV can usually be accomplished mechanically or, in some instances, electronically. Mechanical reduction in the dimensions of the X-ray beam can be achieved by either pre-irradiation (reducing primary radiation dimensions) or post-irradiation (reducing the dimensions of the transmitted radiation, before it is detected) collimation. Currently, most units use adjustable lead shields as primary collimation at the radiation source. For CBCT units employing intensifying screens to detect the image and producing a circular FOV, the diameter of the aperture is reduced. For flat panel detectors providing a rectangular FOV, primary lead collimator shields reduce the height of the scan or vertical dimensions of the volume irradiated and maintain the horizontal cross-sectional volume. On some CBCT units, both vertical and horizontal collimators can be employed. Electronic collimation involves elimination of data recorded on the detector which is peripheral to the area of interest. In this case there is no physical reduction in irradiation of the ROI by physical means – the full FOV is exposed but only the selected region is recorded. Both techniques reduce the amount of data for computational purposes and reduce reconstruction time. However, only pre-irradiation physical collimation of the X-ray beam limits X-radiation exposure to the ROI and results in reduced patient radiation exposure. There are two benefits associated with physical X-ray beam limitation to an anatomic region of interest. First, because less scattered radiation is recorded, images from reduced FOV acquisition are less noisy, of higher contrast with reduced artefacts and provide qualitatively improved image quality for specific diagnostic tasks.[21] More importantly, a reduction in FOV is usually associated with patient dose reductions. This has been reported to range from 25% to 66% depending on machine, type of collimation (vertical and/or horizontal), amount of mechanical collimation and location (maxilla vs. mandible; anterior vs. posterior).[21,31,32] Limitation of the FOV to the smallest ROI necessary for diagnosis using mechanical collimation methods is highly recommended.

Currently available maxillofacial CBCT equipment

CBCT systems can be described according to the orientation of the patient during image acquisition, scan volume acquisition, maximum FOV available and whether additional functionality is available. CBCT units are constructed such that scanning is performed standing, sitting or in the supine position with equipment footprint increasing respectively.

Despite patient orientation, all units provide a head stabilizing mechanism to minimize motion artefact as scan times are often similar to panoramic imaging. Scan volumes may be generated either from a single scan or as a composite of multiple adjacent limited field volumes by digital stitching methods (Fig. 2).

Initially, CBCT units were produced with limited ability to adjust the FOV and were either full maxillofacial units (e.g. NewTom 3G) or small FOV (e.g. early versions of the Morita Accuitimo). The CBCT equipment market has matured such that available units can be grouped into one of three categories based on maximum vertical FOV with most providing a selection of various FOVs: (1) maxillofacial – covers most of the craniofacial skeleton, at least from below the soft tissue of the chin to nasion. Usually greater than 13 cm maximum scan height; (2) dentoalveolar – single or inter-arch ranging from 5 cm to 10 cm incorporating the maxilla and/or mandible; and (3) limited – approximately 5 cm or less vertical height covering localized regions such as a segment of the dental arch or temporomandibular joints.

Selection of FOV is important for restricting the FOV to the ROI to minimize patient radiation exposure. Selection of equipment, and in particular maximum FOV size, should be directed towards the intended diagnostic task. Some CBCT units are capable of high resolution imaging (manufacturer specified 0.076 mm – 0.125 mm voxel resolution) and such high resolution attainment is essential for tasks requiring discernment of fine detail structures and disease processes such as the periodontal space, root resorption and root fracture.

CBCT systems can also be divided into stand-alone or hybrid multi-modal systems that combine digital panoramic radiography with small-to-medium FOV CBCT systems. These units provide substantial cost savings as existing robotic panoramic platforms can be re-engineered and smaller, less expensive detectors can be used.

Image generation and image detection specifications of currently available CBCT systems reflect proprietary variations in image acquisition, detector and image reconstruction (Table 1).

Task specific image display

As CBCT image-capture is inherently digital, image visualization should be by digital display. In addition, unlike other dental radiographic procedures, CBCT acquisition is volumetric in nature and captures 3-D

Table 1. Field of View and voxel size of some commercially available CBCT equipment (data from brochures and/or website)

Model Manufacturer(website)	Field of View (H x D, in mm) Maxillofacial	Dentoalveolar	Limited	Voxel Size (μm)
3D Accuitomo - XYZ Slice View Tomo[a]			30 × 40	125
3D Accuitomo FPD[a]		60 × 60	40 × 40	125
3D Accuitomo 80[a]		80 × 80; 60 × 60	40 × 40	80–160
3D Accuitomo 170[a]	120 × 170; 100 × 140	100 × 100; 80 × 80; 60 × 60; 50 × 170; 50 × 140; 50 × 100	40 × 40	80–250
Aliloth/Aliloth CM[b]		71 × 79	51 × 51	100, 155
Auge Series(Auge X/ZIO/X ZIO)[b]		80 × 79; 80 × 104	55 × 51	100–203
Galileos Comfort[c]	150 × 150 × 150			150, 300
Galileos Compact[c]	120 × 150 × 150			300
GXCB 500[d]		80 × 80; 80 × 140	Height adjustable from 40 to 80.	125–400
GXCB 500 HD[d]		80 × 80; 80 × 140	Height adjustable from 20 to 80.	125–400
i-CAT Classic[e]	130 × 160; 200 × 160	80 × 160; 60 × 160; 60 × 80		120–400
i-CAT Next Generation[e]	170 × 230; 130 × 160	80 × 80	Height (1 mm step) from 20–130 × 160.	125–400
ILUMA LFOV[f]	142 × 211			90–400
ILUMA SFOV[f]		96 × 108		90–400
Kavo 3D eXam[g]	170 × 230; 130 × 160	80 × 80	Height adjustable	125–400
Kavo 3D eXam i[g]		80 × 80; 80 × 140	Height down to 40.	125–400
KODAK 9000 3D[h]			37.5 × 50; 37.5 × 90 × 70	76–200
KODAK 9500 3D[h]	184 × 206	90 × 150		200, 300
NewTom 3G[i]	Sphere 200(D)/150(D)	Sphere 100(D)		200–400
NewTomVGi/ VGi Flex[i]	150 × 150; 120 × 150	80 × 120; 80 × 80; 60 × 60		75–300
NewTom 5G[i]	160 × 180; 120 × 150	80 × 120; 80 × 80; 60 × 60		75–300
Orthophos XG 3D[c]		80 × 80		100, 200
Pax-Duo3D[j]	135 × 150	85 × 120; 85 × 85	50 × 50; 50 × 85	80–300
Pax-Flex 3D[j]		85 × 120 coming soon.	50 × 80; 50 × 50	120, 200
Pax-Reve3D[j]	190 × 150; 150 × 150	80 × 120; 60 × 80	From 50 × 50 to 150 × 150	80–300
PaX Uni3D OS[j]			50 × 50; 50 × 80	200
Pax-Zenith 3D[j]	From 50 × 50 to 190 × 240	From 50 × 50 to 190 × 240	From 50 × 50 to 190 × 240	80–300
Picasso-Trio[j]		70 × 120		200
PreXion 3D[k]		75 × 81	52 × 56	200
ProMax 3D[l]	130 × 140 × 105	80 × 80; 68 × 68;	80 × 40; 68 × 34; 50 × 80; 50 × 40; 42 × 68; 42 × 34	100–400
ProMax 3D Mid[l]	160 × 160; 160 × 90	90 × 160; 90 × 90; 75 × 75; 70 × 70; 60 × 60	50 × 160; 50 × 90; 42 × 75; 50 × 70; 42 × 60; 70 × 40; 60 × 34; 50 × 40; 42 × 34	100–600
ProMax 3D Max[l]	260 × 230; 160 × 230; 160 × 130; 136 × 110; 130 × 130; 130 × 100	110 × 110; 110 × 85; 90 × 130; 75 × 110; 90 × 100; 75 × 85	55 × 130; 50 × 110; 55 × 100; 50 × 85; 55 × 50; 50 × 42	100–600
ProMax 3Ds[l]	130 × 90 × 60		80 × 50; 68 × 42; 50 × 50; 42 × 42	100, 200
Scanora 3D/ENT[m]	130 × 145	75 × 145; 75 × 100; 60 × 60		133–350
Scanora 3Dx[m]	240 × 170; 180 × 170; 135 × 170	80 × 100	50 × 100; 50 × 50	100–500
SkyView 3D[n]	Sphere 150(D)/110(D)	Sphere 70(D)		160–330
Suni 3D[o]			50 × 50; 50 × 80	200
Suni 3D HD[o]			50 × 50	80, 125
Veraviewepocs 3D[a]		80 × 80	40 × 40; 80 × 40	125
Veraviewepocs 3De[a]			40 × 40; 80 × 40	125

[a]J. Morita Mfg. Corp., Kyoto, Japan (http://www.jmorita-mfg.com/en/en_products_diagnostics.htm).
[b]Asahi Roentgen Ind. Co., Ltd. Kyoto, Japan (http://www.asahi-xray.co.jp/global/products).
[c]Sirona Dental Systems, Charlotte, NC, USA (http://www.sirona.com/ecomaXL/index.php?site=SIRONA_COM_galileos)
[d]Imaging Sciences - Gendex, Chicago, IL, USA (http://www.gendex.com/US/Products/Cone-Beam-3-D-Imaging.aspx).
[e]Imaging Sciences International, Hatfield, PA, USA (http://www.imagingsciences.com/products).
[f]IMTEC, a 3M Company, Ardmore, OK, USA (http://www.3d-roentgen.ch/pdf/IMTEC_Iluma_e.pdf).
[g]Imaging Sciences - KaVo Dental Corp., Biberach, Germany (http://www.materialise.com/materialise/view/en/3373888-KaVo.html).
[h]KODAK Dental Systems, Carestream Health Rochester NY, USA (http://www.carestreamdental.com/en/digital-imaging/3d-imaging).
[i]QR SRL Via Silvestrini, Verona Italy (http://www.qrverona.it/index.php?rel=products&lan=eng).
[j]Vatech, Giheung-gu, Korea (http://www.vatechamerica.com/products).
[k]PreXion, Inc., San Mateo, CA, USA/ The Yoshida Dental Mfg. Co., Ltd, Tokyo, Japan. (http://www.prexion.com/dental/index.html/ http://www.yoshida-net.co.jp/en/products/x-ray%20systems/ct/finecube/p02.html).
[l]Planmeca Oy, Helsinki, Finland (http://www.planmeca.com/en/imaging).
[m]SOREDEX, Tuusula, Finland (http://www.soredexusa.com).
[n]My-Ray Dental Imaging, Cefla Dental Group, Imola, Italy (http://www.my-ray.com/site/page.wplus?ID_COUNT=skyview&LN=2).
[o]Suni Medical Imaging, Inc. San Jose, CA, USA (http://www.suni.com/usa/products/Suni3D_HD.aspx).

information. Therefore, to enable visualization of increasing digital information contained within the imaging volume, the interpretation should move from static hard copy (printed) to software-assisted volumetric review. This demands that image display for interpretation be dynamic and facilitated by the use of appropriate application of software and task specific protocol formatting.

The default presentation of the dataset by most visualization software is usually as a series of 2-D contiguous interrelational images at a thickness defaulted to the native resolution in three orthogonal planes (axial, sagittal and coronal). In principle, CBCT data should be considered as a volume to be explored from which other images are extracted. Mechanically, this involves the application of a protocol or series of logical sequential steps to optimize image presentation.

We have developed a technique involving three stages, which in our experience, provides an efficient and consistent systematic methodological approach to CBCT image display prior to image interpretation.

(1) **Correct the data.** Because reconstruction of CBCT data is performed natively using a personal computer, initial adjustment should comprise data reorientation such that the patient's anatomic features are realigned. This should be task specific. For example, in craniofacial analysis the volumetric dataset should be adjusted such that Frankfort horizontal (FH, i.e. nasion-orbital) is parallel to the floor and the mid-sagittal plane is perpendicular to FH. Next, the dataset should be optimized for display by the adjustment of greyscale brightness levels, establishment of a contrast range and the application of specific filters (e.g. interpolation, sharpen noise), all directed towards favouring cortical and trabecular bone. After these adjustments then secondary algorithms (e.g. annotation, measurement and magnification) can be applied with confidence.

(2) **View the data.** Because of the large number of component orthogonal images in each plane it is necessary to review each series dynamically by scrolling through the orthogonal image stack. This is referred to as a 'cine' or 'paging' mode. It is recommended that scrolling should be performed cranio-caudally (i.e. from 'head-to-toe') and then in reverse, slowing down in areas of greater complexity (e.g. temporomandibular joint articulations). This scrolling process should then be repeated both in the coronal and sagittal planes. Detection of soft tissue calcifications can be improved by finally repeating this process using an approximately 10 mm slab thickness combined with a maximum intensity profile (MIP) setting (see later).

(3) **Display the data.** CBCT software provides an almost infinite and perhaps bewildering number of visualization options, each directed towards highlighting specific components of the volumetric dataset. Protocols incorporating FOV scan exposure parameters and display modes (Fig. 8) should be applied selectively to highlight anatomic features or functional characteristics within a specific diagnostic task. It is beyond the purpose of this article to describe specific display protocols, however selection should be based on applying thin sections for detail and thicker sections to demonstrate relationships. Because of the isotropic nature of acquisition, the volumetric dataset can be sectioned non-orthogonally to provide non-axial 2-D planar images referred to as multiplanar reformations (MPR). In addition, the thickness of such planar images can be increased. MPR modes include oblique, curved planar reformation providing 'simulated' distortion-free panoramic images and serial transplanar reformation (providing cross-sections), all of which can be used to highlight specific anatomic regions and facilitate diagnostic tasks. This is important given the complex structure of the maxillofacial region. Because of the large number of component orthogonal images in each plane and the difficulty in relating adjacent structures, two methods have been developed to visualize adjacent voxels (Fig. 9).

(a) **Ray sum or ray casting.** An MPR image can be increased in thickness by increasing the number of adjacent voxels. This creates an image 'slab' that represents a specific narrow volume of the patient, referred to as a *ray sum*. Full thickness

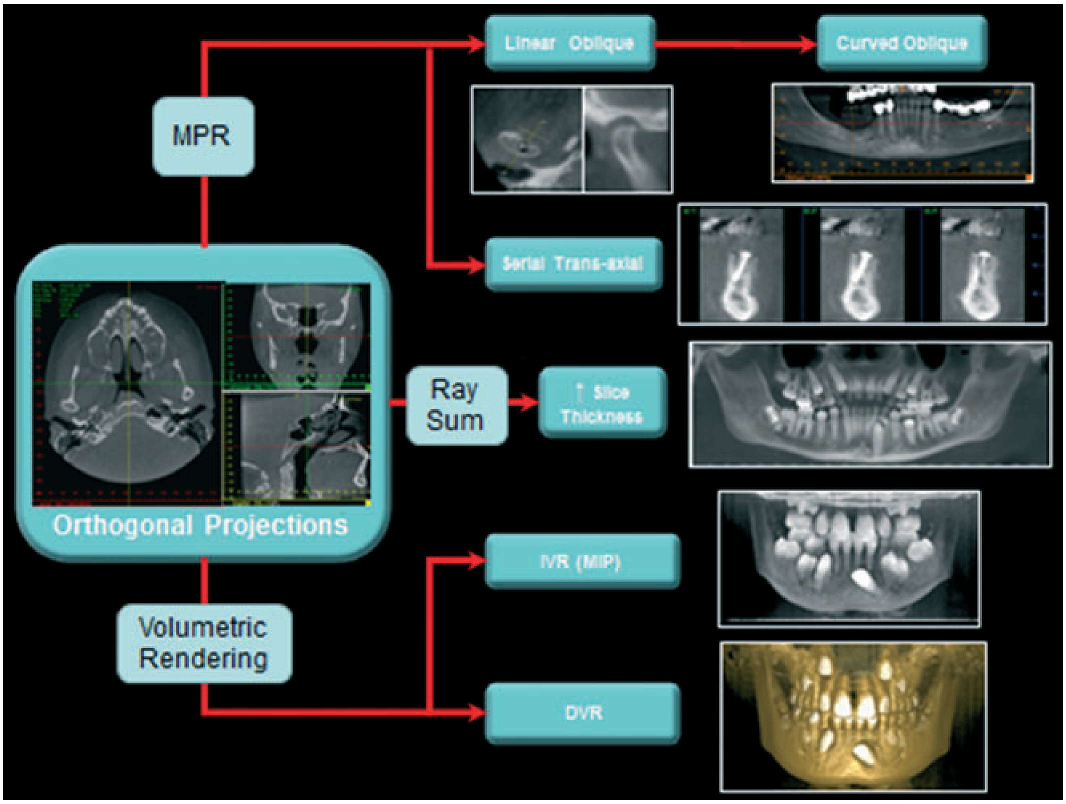

Fig 8. Display mode options of CBCT volumetric data. Display modes can be divided into three categories: (a) multiplanar reformatted (MPR) consisting of linear, curved oblique and serial trans-axial images; (b) ray sum comprising images of increased section thickness; and (c) volumetric images consisting of indirect volume rendering (IVR), the most common of which being maximum intensity projection (MIP) and direct volume rendering (DVR).

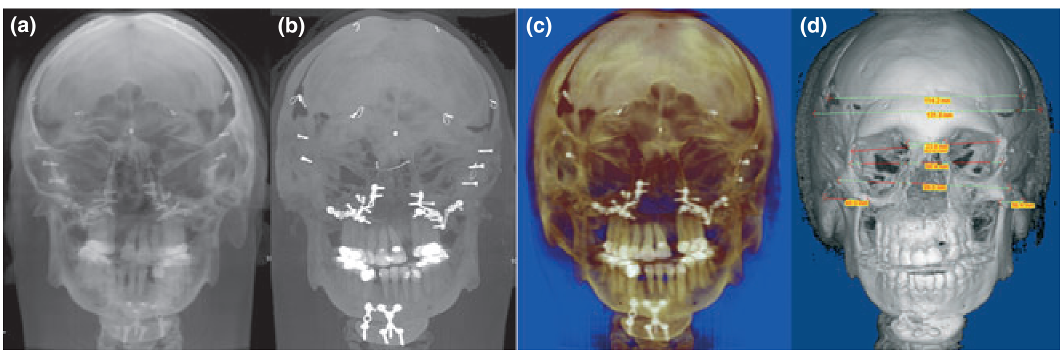

Fig 9. Comparison of 3-D visualization techniques applied to CBCT dataset of a patient with a craniofacial deformity: ray sum (a), maximum intensity projection (b) and 3-D computer-generated modelling including volumetric transparent (c) and shaded surface display (d). 3-D cephalometric measurements can be performed interactively on the volumetric representations (d). Volumetric dataset acquired with extended field of view iCAT (Imaging Sciences International, Hatsfield, PA, USA) and all reconstructions generated using Dolphin 3D (Dolphin Imaging, Chatsworth, CA, USA).

ray sum images can be used to generate simulated projections such as lateral cephalometric images. Unlike conventional radiographs, these ray sum images are without magnification and are undistorted. However, this technique uses the entire volumetric dataset and interpretation suffers 'anatomic noise', superimposition of multiple structures, also inherent in simple transmission radiographs.

(b) **Volume rendering.** Volume rendering refers to techniques which allow the visualization of volumetric data by selective display of voxels within a dataset. Two specific techniques are commonly used. Indirect volume rendering (IVR) is a complex process, requiring selection and graphic representation of a range of the intensity greyscale levels of the voxels (called segmentation). Such a process provides a volumetric surface reconstruction with depth. Direct volume rendering (DVR) is the selection of an arbitrary threshold of voxel intensities, below or above which all grey values are eliminated. The most common DVR technique is MIP. MIP visualizations are achieved by evaluating each voxel value along an imaginary projection ray from the observer's eyes within a particular volume of interest and then representing only the highest value as the display value. Voxel intensities that are below an arbitrary threshold are eliminated.

Interpretation of CBCT images

It is the professional duty of a practitioner who operates a CBCT unit or requests a specific CBCT study to provide information on the imaging findings based on examination of the entire image dataset. In some jurisdictions this is also legally mandatory, either for reimbursement from third-party health insurance payers or to maintain professional medical liability protection. An opinion expressed by some has been that the user is not responsible for the radiologic findings beyond those needed for a specific task (e.g. implant treatment planning). Professional bodies in both the United States[18] and Europe[33] vigorously oppose this position.

Radiologic interpretation is predicated on a thorough knowledge of CT anatomy for the entire acquired image volume, anatomic variations and observation of abnormalities. It is imperative that all image data be systematically reviewed for disease. Competency in interpretation of both anatomic and pathologic findings on CBCT images varies depending principally on practitioner experience and the FOV of the scan. Qualified specialist oral and maxillofacial radiologists may be able to assist diagnostically when practitioners are unwilling to accept the responsibility to review the whole exposed tissue volume.

It is important to recognize that CBCT imaging comprises two components: the generation of task specific images and an interpretation report. Often patient diagnosis may be complex and management may involve numerous practitioners. Therefore, an interpretation report serves as the optimal method of communication of interpretation findings for CBCT.

Currently, there is no consensus on the specific requirements for CBCT reporting. However, guidelines for comparable reporting of MSCT images are available and should be consulted.[34,35] Within this framework, and based on dedicated CBCT imaging experience dating to 2004, the authors suggest that the following outline form the basis for CBCT reporting:

(1) **Patient information.** This section should include pertinent information to identify the patient and provide possible relevant demographic data. This would include the patient name or other identifier, gender, date of birth or age.

(2) **Scan information.** This section provides the when, where, why, and how for the CBCT procedure. This would include succession number, date the scan was performed, date the report was generated, the location of the facility, the equipment used, scan parameters, the referring practitioner's name, rationale for the procedure and images provided. In addition, information should be provided on any problems encountered during the procedure (e.g. patient motion)

(3) **Radiologic findings.** This section should be subdivided into general imaging findings, specific radiologic findings pertinent to the imaging rationale and incidental findings. General imaging findings should include reference to the dental status including specific missing teeth, restorative status, root canal filled teeth, periapical lesions, general alveolar bone status and status of edentulous regions. Specific findings should use precise anatomic, pathologic and radiologic terminology to accurately describe gnathic or temporomandibular joint features regarding the region of interest. In the maxilla, the paranasal sinuses should be examined with particular reference to the characteristics of any opacification, if present. Finally, depending on the FOV of the dataset, the dataset should then be reported 'head-to-toe', reflecting the approach previously described. Incidental findings should comment on significant conditions observed in non-gnathic structures including the cranial cavity (e.g. physiologic and pathologic calcifications), the base of the skull including the auditory apparatus, the naso- and oropharyngeal airway spaces, the cervical spine and the soft tissues of the neck.

(4) **Radiologic impression.** Either a definitive or a differential diagnosis should be provided, whichever is appropriate. In this section the radiologic findings should be correlated to patient presentation and address or answer any pertinent clinical issues raised in the request for the imaging examination. If available, findings should be compared to previous examinations or reports. Finally, recommendations for follow-up or additional diagnostic or clinical studies should be suggested, as appropriate, to clarify, confirm or exclude the diagnosis.

CONCLUSIONS

The application of CBCT theory to produce equipment dedicated for use in dentistry has reached maturity since its commercial introduction more than a decade ago.

Numerous manufacturers produce a large selection of CBCT units all capable of providing accurate, submillimetre resolution images in formats enabling volumetric visualization of the osseous structures of the maxillofacial region. Further applications and increasing availability of this technology will extend maxillofacial CBCT imaging from diagnosis to image guidance of operative and surgical procedures. CBCT will undoubtedly affect the expected standards of care, and this has implications for increased practitioner responsibility both in the performance, optimal visualization and interpretation of volumetric datasets.

REFERENCES

1. Ziesdes des Plantes BG. Selected works of BG Ziesdes des Plantes. Amsterdam: Excerpta Medica, 1973:137–140.
2. Webber RL, Horton RA. Tuned-Aperture Computed Tomography: Theory and Application in Dental Radiology. In: Advances in Maxillofacial Imaging. Farman AG, Ruprecht A, Gibbs SJ, Scarfe WC, eds. Amsterdam: Elsevier Science BV, 1997:359–366.
3. Hounsfield GN. Nobel Lecture. 8 December 1979. Computed medical imaging. J Radiol 1980;61:459–468.
4. Cormack AM. Early two-dimensional reconstruction (CT scanning) and recent topics stemming from it. Nobel lecture. 8 December 1979. J Comput Assist Tomogr 1980;4:658–664.
5. Goldman LW. Principles of CT and CT Technology. J Nucl Med Technol 2007;35:115–128.
6. Robb RA, Lent AH, Gilbert BK, Chu A. The dynamic spatial reconstructor: a computed tomography system for high-speed simultaneous scanning of multiple cross sections of the heart. J Med Syst 1980;4:253–288.
7. Robb RA. The dynamic spatial reconstructor: an x-ray video-fluoroscopic CT scanner for dynamic volume imaging of moving organs. IEEE Trans Med Imaging 1982;1:22–33.
8. Sukovic P. Cone beam computed tomography in craniofacial imaging. Orthod Craniofac Res 2003;6(Suppl 1):31–36.
9. Hayakawa Y, Sano T, Sukovic P, Scarfe WC, Farman AG. Cone beam computed tomography – a paradigm shift for clinical dentistry. Nippon Dental Review 2005;65:125–132.
10. Farman AG, Levato CM, Scarfe WC. A primer on cone beam computed tomography. Inside Dentistry 2007;3:90–93.
11. Scarfe WC, Farman AG. Cone beam computed tomography: a paradigm shift for clinical dentistry. Australasian Dental Practice 2007;Jul-Aug:102–110.
12. Feldkamp LA, Davis LC, Kress JW. Practical cone-beam algorithm. J Opt Soc Am A 1984;1:612–619.
13. Wischmann H-A, Luijendijk HA, Meulenbrugge HJ, Overdick M, Schmidt R, Kiani K. Correction of amplifier nonlinearity, offset, gain, temporal artefacts, and defects for flat-panel digital imaging devices. In: Medical Imaging 2002. Physics of Medical Imaging. Antonuk LE, Yaffe MJ, eds. Proceedings of SPIE Volume 4682. San Diego, CA: SPIE, 2002:427–437.
14. Grangeat P. Mathematical framework of cone beam 3D reconstruction via the first derivate of the Radon transform. Mathematical Methods in Tomography. In: Herman GT, Louis AK, Natterer F, eds. Berlin: Springer, 1991:66–97.
15. Scarfe WC, Farman AG, Sukovic P. Clinical applications of cone-beam computed tomography in dental practice. J Can Dent Assoc 2006;72:75–80.
16. Farman AG. Image guidance: the present future of dental care. Pract Proced Aesthet Dent 2006;18:342–344.
17. Koyama S, Aoyama T, Oda N, Yamauchi-Kawaura C. Radiation dose evaluation in tomosynthesis and C-arm cone-beam CT examinations with an anthropomorphic phantom. Med Phys 2010;37:4298–4306.
18. Carter L, Farman AG, Geist J, *et al.* American Academy of Oral and Maxillofacial Radiology executive opinion statement on performing and interpreting diagnostic cone beam computed tomography. Oral Surg Oral Med Oral Pathol Oral Radiol Endod 2008;106:561–562.
19. Kau CH, Bozic M, English J, Lee R, Bussa H, Ellis RK. Cone-beam computed tomography of the maxillofacial region – an update. Int J Med Robot 2009;5:366–380.
20. International Commission on Radiation Protection. Recommendations of the International Commission on Radiation Protection, ICRP Publication 26. Ann ICRP 1977;1:3.
21. Qu XM, Li G, Ludlow JB, Zhang ZY, Ma XC. Effective radiation dose of ProMax 3D cone-beam computerized tomography scanner with different dental protocols. Oral Surg Oral Med Oral Pathol Oral Radiol Endod 2010;110:770–776.
22. Lofthag-Hansen S, Thilander-Klang A, Gröndahl K. Evaluation of subjective image quality in relation to diagnostic task for cone beam computed tomography with different fields of view. Eur J Radiol 2011;80:483–488.
23. Sur J, Seki K, Koizumi H, Nakajima K, Okano T. Effects of tube current on cone-beam computerized tomography image quality for presurgical implant planning in vitro. Oral Surg Oral Med Oral Pathol Oral Radiol Endod 2010;110:e29–33.
24. Kwong JC, Palomo JM, Landers MA, Figueroa A, Hans MG. Image quality produced by different cone-beam computed tomography settings. Am J Orthod Dentofacial Orthop 2008;133:317–327.
25. Chen L, Shaw CC, Altunbas MC, Lai CJ, Liu X. Spatial resolution properties in cone beam CT: a simulation study. Med Phys 2008;35:724–734.
26. Bryant JA, Drage NA, Richmond S. Study of the scan uniformity from an i-CAT cone beam computed tomography dental imaging system. Dentomaxillofac Radiol 2008;37:365–374.
27. Nackaerts O, Maes F, Yan H, Couto Souza P, Pauwels R, Jacobs R. Analysis of intensity variability in multislice and cone beam computed tomography. Clin Oral Implants Res 2011;22:873–879.
28. Lagravère MO, Fang Y, Carey J, Toogood RW, Packota GV, Major PW. Density conversion factor determined using a cone-beam computed tomography unit NewTom QR-DVT 9000. Dentomaxillofac Radiol 2006;35:407–409.
29. Lagravère MO, Carey J, Ben-Zvi M, Packota GV, Major PW. Effect of object location on the density measurement and Hounsfield conversion in a NewTom 3G cone beam computed tomography unit. Dentomaxillofac Radiol 2008;37:305–308.
30. Mah P, Reeves TE, McDavid WD. Deriving Hounsfield units using grey levels in cone beam computed tomography. Dentomaxillofac Radiol 2010;39:323–335.
31. Roberts JA, Drage NA, Davies J, Thomas DW. Effective dose from cone beam CT examinations in dentistry. Br J Radiol 2009;82:35–40.
32. Ludlow JB, Davies-Ludlow LE, Brooks SL, Howerton WB. Dosimetry of 3 CBCT devices for oral and maxillofacial radiology: CB Mercuray, NewTom 3G and i-CAT. Dentomaxillofac Radiol 2006;35:219–226. Erratum in: Dentomaxillofac Radiol 2006;35:392.
33. Horner K, Islam M, Flygare L, Tsiklakis K, Whaites E. Basic principles for use of dental cone beam computed tomography: consensus guidelines of the European Academy of Dental and Maxillofacial Radiology. Dentomaxillofac Radiol 2009;38:187–195.
34. American College of Radiology. ACR Practice Guideline for Performing and Interpreting Diagnostic Computed Tomography.

Available at: 'http://www.acr.org/SecondaryMainMenuCategories/quality_safety/guidelines/dx/ct_performing_interpreting.aspx'. Accessed 15 June 2011.

35. American College of Radiology. ACR Practice Guideline for Communication: Diagnostic Radiology. Available at: 'http://www.acr.org/secondarymainmenucategories/quality_safety/guidelines/dx/comm_diag_rad.aspx'. Accessed 15 June 2011.

Address for correspondence:
Professor William C Scarfe
The University of Louisville
School of Dentistry
Radiology and Imaging Science
Department of Surgical and Hospital Dentistry
Room 149F
501 South Preston Street
Louisville
Kentucky 40292
USA
Email: wcscar01@louisville.edu